

Sizing for endovascular aneurysm repair: clinical evaluation of a new automated three-dimensional software

Adrien Kaladji ^{1 2 3 *}, Antoine Lucas ^{1 2 3}, Gaëlle Kervio ^{1 3}, Pascal Haigron ¹, Alain Cardon ^{2 3}

¹ LTSI, Laboratoire Traitement du Signal et de l'Image INSERM : U642, Université de Rennes I, Campus de Beaulieu, 263 Avenue du Général Leclerc - CS 74205 - 35042 Rennes Cedex,FR

² Service de Chirurgie Vasculaire CHU Rennes, Hôpital Sud, 35000 Rennes,FR

³ CIC-IT, Dispositifs Diagnostic et Thérapeutiques CHU Rennes, INSERM : CICIT 804, 2 Rue Henri de Guilloux,FR

* Correspondence should be addressed to: Adrien Kaladji <kaladrien@hotmail.fr >

Abstract

Purpose

To assess the reproducibility and accuracy of the sizing procedure prior to aortic endograft implantation using new sizing automated software compared to standard radiological procedures.

Methods

Based on original spiral-computed tomography images, the sizing of 32 patients with abdominal aortic aneurysm (AAA) treated by endovascular aneurysm repair (EVAR) was retrospectively compared. The first sizing was performed by a radiologist using a standard workstation (General electrics) and software (Advanced vessel analysis). The second was performed twice by two surgeons using a personal computer with automatic three-dimensional sizing software (Endosize, Therenva). All diameters and lengths required prior to EVAR were measured (17 items). Additionally, thirteen qualitative criteria regarding EVAR feasibility, including neck length, were compared. Intra- and interobserver variability with Endosize, as well as the variability between the two measurement methods were analyzed using the intraclass correlation coefficient (ICC) and Bland and Altman's method. Qualitative variables were analyzed using Fischer's exact test and kappa coefficient.

Results

Intra-observer variability with Endosize proved to be efficient. None of the ICCs were lower than 0.9, and more than 90% of the absolute differences between two measurements were less than 2mm. Inter-observer variability with Endosize was assessed in a similar manner. Measurement variability of vessel diameters was less marked than that of vessel lengths. This trend was observed for all data sets. Comparison of the two measurement methods demonstrated a good correlation (minimum ICC=0.697; maximum ICC=0.974), though less so than that observed using Endosize. Mean time consumption using Endosize was 13.1+/-4.53 minutes (range: 7.2-32.7). Analysis of the alarm sets demonstrated a high agreement between observers (kappa coefficient=0.81).

Conclusion

Sizing using the Endosize software is as reliable as conventional radiological procedures. Sizing by surgeons using an automated, user-friendly, and mobile tool appears to be reproducible.

Author Keywords Sizing ; EVAR ; endovascular intervention ; computed tomography angiography ; workstation ; post-processing image treatment ; preoperative measurements

INTRODUCTION

The sizing, which is the first step of endovascular aneurysm repair (EVAR), is essential for a successful procedure. Several sizing methods^{1,2} have been assessed, using highly sophisticated and expensive radiological workstations and software. Surgeons must be able to control this first step using reliable software, with results that are as accurate as those obtained at radiological workstations. For surgeons using this software, preoperative navigation within the vessels and accurate measurements are the primary objectives, enabling them to accurately plan an EVAR. To our knowledge, there is little data on automated software testing in a clinical evaluation context. This study aimed to assess whether the sizing procedure using automated three-dimensional (3D) sizing software, which had been developed in our clinical investigation and technological innovation center, was as accurate and reproducible as that performed at a radiological workstation.

METHODS

In total, 32 patients (29 men, 3 women; mean age: 74.9 +/-9.4) with abdominal aortic aneurysm (AAA) and treated by endovascular AAA repair (EVAR) were studied retrospectively. They were randomly assigned to EVAR procedure between 2006 and 2007. Patients were selected for EVAR based on clinical and morphological criteria (Table 1).

Measurements

All patients were evaluated using spiral computed tomography angiography (CTA) prior to EVAR. All imaging examinations were performed on a multislice CT scanner (General Electric Medical Systems, Milwaukee, Wisconsin, LightSpeed16). Parameters for the acquisitions were 1.25mm slice thickness, 120 kVp, and 215–360 mA tube current. Imaging was initiated after administering 120mL of low-osmolar iodinated contrast agent (Hexabrix, iodine concentration 320mg/ml). Soft tissue window settings with a width of 400HU and a center of 40HU were applied.

Quantitative variables studied (Fig. 1) included the largest and smallest diameter on CT slices on the first slice distal to the lowermost renal artery (D1a), 15mm below this landmark (D1b), healthy neck end (D1c), as well as left (D2) and right (D3) distal primitive iliac arteries. Maximal AAA diameter (DAAA) and smallest diameter of left (Lmin) and right (Rmin) external iliac arteries were also measured. Length measurements included proximal aortic neck (NL), length between the lowermost renal artery and aortic bifurcation (L1), as well as left (L2) and right (L3) common iliac arteries.

Qualitative variables, referred to as “alarms”, were defined as morphological features of the aneurysm which could change the therapeutic strategy or draw the surgeon’s attention to potential technical difficulties during the procedure. These variables were NL \leq 15mm (V1), D1a \leq 18 mm or \geq 32 mm (V2), reverse taper neck (or difference between D1a and D1c \geq 25%) (V3), bony-sharp neck \geq 60° (V4), aortic bifurcation (D4) \leq 20 mm (V5), L2 \leq 10 mm (V6), L3 \leq 10 mm (V7), Lmin \leq 7.5 mm (V8), Rmin \leq 7.5 mm (V9), D2 \geq 20 mm (V10), D3 \geq 20 mm (V11), left iliac tortuosity (V12), and right iliac tortuosity (V13). These data sets were characterized as present or absent.

In addition, stent graft type (aorto-uni-iliac or aorto-bi-iliac) and predicted complementary procedures or complications which arose during EVAR were reported.

Image Analysis

The first sizing was performed by an interventional radiologist. Original contrast-enhanced CT images were electronically transferred to a General Electrics workstation, and measurements of aorto-iliac lengths and diameters were carried out using advanced vessel analysis (AVA) software. These measurements were considered as references for the procedure planning. Thereafter, a vascular surgeon, who was blinded to all radiological results, carried out the sizing of the endograft after importing the same scan data. This sizing was performed using Endosize (Therenva, Rennes), a 3D sizing software tool that had been optimized to run on a conventional personal computer (PC). A 2.4 GHz processor and 2 Go random access memory (RAM) were components of the surgeon’s PC. Measurements with Endosize were repeated twice (Sizing 1 and 2) by two vascular surgeons (Surgeon 1 and 2), separated by a 2-week time interval. Each sizing was recorded. Endosize operated in four steps:

- CT data loading and visualization: Two-dimensional slice views and smooth volume rendering view were obtained.
- Data processing: The vessel lumen and centerline extraction required viewing the aortic structure in 3D. The image analysis process was based on a combination of boundary-based and region-based segmenting algorithms including morphological operations to automatically remove connection between the vasculature of interest (aorto-iliac structure) and bone structures (such as vertebra), as well as to determine the centerlines of vascular branches^{3,4,5}. Moreover, a powerful and optimized volume-rendering process exploiting graphics processing unit computation performances was implemented in order to visualize three-dimensional vascular geometry. In addition to this, 3D vessel description scheme, as well as reformatted CT slices and contours of the vessel lumen were computed along the vessels’ curvilinear axes. Only one parameter could intuitively be adjusted during the data processing step, which determined the discrete volume (voxels) contained in the vessel lumen. The computation time for data processing and rendering, consecutive to a new adjustment of this parameter, took approximately 1 second, which was compatible with using interactive software. Moreover, as the default value of this analysis parameter had been settled for AAA CTA observations, in most cases no modifications were needed. The graphics user interface thus allowed for linking the anatomical features of the aorto-iliac structure (geometry and parietal quality) to those of the stent graft, while the user (vascular surgeon or interventional radiologist) remained in control of the decision-making process.
- Semi-automatic measuring (Fig. 2): Useful lengths and diameters taken on the vessel centerlines were automatically obtained after a simple interactive step consisting in a three-dimensional point picking sequence. To this end, eight points were required, corresponding to the suprarenal aorta, infrarenal fixation site, healthy neck end, aortic bifurcation, left iliac bifurcation, right iliac bifurcation, left external distal site, and right external distal site. In the next step, while the length and diameter measurements were proposed by the software, the user had to control the measurements’ accuracy on a separate window showing the slice (perpendicular to the centerline) used by the

software to assess the diameters. The software proposed inner-to-inner diameter measurements. Surgeons were given the option of including a thrombus in the measurements, with an adjustable parameter for an enlarged area of measurement of interest. In the case of disagreement, the user could easily adjust the measurement.

- Sizing report (Fig. 3): The feasibility of the procedure was defined by the aforementioned alarms.

Statistical Analysis

Quantitative and qualitative variables were analyzed separately by several methods. For quantitative variables, correlation was assessed using the intraclass coefficient correlation (ICC), and variation between the data sets was compared by calculating the mean pair difference for each data point and averaging them for the dataset comparison. According to the method described by Bland and Altman, limits of agreement were calculated (for each point: mean difference between observers \pm the standard deviation multiplied by 1.96). Mean time consumption for sizing was compared using the non-parametric Wilcoxon signed rank test (intra- and inter-observer). Qualitative variables were analyzed using Fischer's exact test and kappa coefficient. $P < 0.05$ was considered significant. Complete agreement was defined as 1.0.

RESULTS

Quantitative Data

Intra-observer

All ICCs were above 0.9, except for and mean differences were less than 1mm for all diameters measured (Table 2 , Fig. 4). Differences were more pronounced for length measurements, though still less than 2mm, with similar trends observed for absolute differences. For all diameters, at least 95% of absolute differences were less than 2mm, and in no case did they exceed 5mm. Absolute differences in lengths were more pronounced, exceeding 5mm in some of the cases. Mean time consumption for sizing (Table 5) did not exceed 15 minutes. There was no statistical difference in time consumption for the two sizing by each surgeon (p value from Wilcoxon test for surgeon 1 for the comparison between sizing 1 and 2 was 0.215 for surgeon 1, and 0.473 for surgeon 2).

Inter-observer

All ICCs were above 0.9 except for D1a max (0.891) (table 4 , Fig. 4). In addition, mean differences were more pronounced for lengths than diameters. The maximum mean difference was 2.051mm for L1 (length between renal arteries and aortic bifurcation), with 92.2% of absolute differences in diameters being lower than 2mm, and 100% lower than 5mm. Absolute differences for lengths were also more marked (in the worst scenario, 68.8% were lower than 2mm for L1). For the first sizing, there was no statistical difference between surgeons 1 and 2 ($p=0.401$), in contrast to the second sizing, where a significant difference was observed ($p=0.001$).

Radiological workstation/Endosize

Six items presented an $ICC \geq 0.9$, seven items an ICC between 0.8 and 0.9, and three items an ICC between 0.7 and 0.8 (minimum for D1a min, $ICC=0.697$) (Table 4 , Fig. 4 , Fig. 5a-c). The maximum mean difference was 3.974mm (L1). For more than 50% of length measurements, absolute differences were above 2mm (versus 70.2% for diameters). Mean time consumption for sizing during the study was 13.1 ± 4.53 minutes (minimum 7.2; maximum 32.7).

Qualitative Data

Regarding EVAR alarms, the radiologist emitted 41 alarms and the surgeon 37 alarms. Fischer's exact test revealed no significant difference between the alarms emitted by the radiologist and surgeon. Overall, 87% of the alarms emitted by the radiologist were the same as those emitted by the surgeon, while 94% of the alarms emitted by the surgeon were the same as those emitted by the radiologist. Analysis of the alarm sets reveals a high agreement between observers (kappa coefficient=0.81).

Type of stent graft

Five patients, three with an aortic bifurcation stenosis and two with AAA and iliac aneurysm, were treated using an aorto-uni-iliac stent graft with femoro-femoral cross bypass (Table 6). For three patients (A, B, C), V5 alarm (aortic bifurcation ≤ 20 mm) was emitted by the radiologist and surgeon. Patients A and B had their endograft implanted on the right side, and patient C on the left side. For patients A and B, no other alarm was emitted by either the radiologist or surgeon (regarding iliac status). For patient C however, both of them had emitted the V8 and the V9 alarms (left and right external iliac stenosis), and an angioplasty was performed on the right side prior to EVAR. For patients D and E, no aortic bifurcation stenosis was detected by either the radiologist or surgeon. For patient D, V9 alarm (right external iliac stenosis) was emitted by both the radiologist and surgeon, while V11 alarm (right primitive iliac aneurysm) was emitted by radiologist alone. The endograft was implanted on the left side with a ligation of the right primitive iliac artery (diameter of the right primitive iliac artery by the surgeon was 13 and 22mm. For the last patient, only the V10 alarm (left primitive iliac aneurysm) was emitted by both the radiologist and surgeon (about iliac level).

EVAR procedure

Predicted complementary procedures during EVAR included two hypogastric coverages: one on the right side where a right distal primitive iliac aneurysm was identified by both observers, and the other on the left side where a bilateral distal primitive iliac aneurysm was identified. Non-predicted complementary procedures included an iliac stent graft extender module where an iliac tortuosity was detected; Type 1a endoleak treated with a Palmaz stent, where any alarms about the neck were emitted; a right external iliac dissection, treated using a bypass, following an aorto-uni-iliac stent graft implanted on the right side, where no stenosis along the artery was detected by either the radiologist or surgeon.

DISCUSSION

Based on these findings, sizing using Endosize software appears to be a reliable and reproducible tool. Others studies^{1, 2, 6} have evaluated different methods of sizing by examining variability, and their conclusions suggest that both intra- and inter-observer variability were not satisfactory. Nevertheless, there are some methods available to lower this variability, notably Endosize software. The use of 3D reconstruction based on spiral CT images to perform a reliable sizing is one of the principle methods^{7, 8, 9, 10}. Extracting a centerline is essential in order to avoid parallax error^{11, 12, 13, 14}. Fukhara et al.¹⁵ established another method, consisting in vessel lumen and thrombus separation using in Endosize. Without corrections, Endosize calculates inner-to-inner diameters, as 3D representation is taken from the vessel lumen. Extraction process is not optimized to perform a 3D representation with different components of aortic wall. However, each parameter must be controlled, and the user has the option to include thrombus (or calcification) measurements. This is possible due to the slice which is perpendicular to centerline, and a tool adjusting the area of interest in measurement, which detects lumen, thrombi, and calcifications. Moreover, in this study, there was no case of severe thrombus in the aortic neck or at iliac fixation sites, as these are considered to be contraindications to EVAR (exclusion criteria). Thrombus within the aneurysm does not influence the planning of EVAR. We believe that when detecting a thrombus, it is essential to schedule navigation within the vessel during the procedure, and that this is accurately assessed with multiplanar reformatted slices.

Regarding the intra-observer variability, reproducibility proved efficient. Automatic tracking appears to provide the same measurements as long as the eight points placed in aorto-iliac representation are at the same location. The variability noted between observers is due to discrepancies in the placement of these points, which explains why ICCs and variations were more pronounced for lengths.

Differences between the two measurement methods were more pronounced, particularly for lengths, but still appear to be widely acceptable. Indeed, the point defining aortic bifurcation is a slightly higher when using Endosize than AVA. This point corresponded to the intersection with the centerline of iliac arteries, while in the radiologist's measurements, it was located on the real point in the arterial wall of the aortic bifurcation. One limitation of the present study was that the same observer's variability when using the two methods could not be studied due to the retrospective design of the study.

The feasibility of EVAR, as represented by the study's qualitative variables, was similarly evaluated by both the radiologist and surgeon. For the five aorto-uni-iliac endografts implanted, an appropriate alarm was emitted each time by the Endosize software except in the case of patient D. The radiologist identified an iliac aneurysm, whereas the Endosize software did not emit the appropriate alarm as the alarm cut-off was 20mm. However, for this patient, iliac artery measurements of 13mm and 22mm (average 17.5mm) did reveal an iliac ectasia. Predicted complementary procedures were identified by Endosize as well as the radiologist. Nonetheless, observers did not anticipate all complications, suggesting that CTA analysis prior to EVAR should not be limited to sizing the AAA, but also requires special attention directed at the quality of the aortic wall (calcifications, thrombus...).

While several sizing software for EVAR are used by radiologists and surgeons, only a few studies have reported on the assessment of software aimed specifically at surgeons, and which is as reliable as conventional radiological software. Neri et al.¹⁶ reported on an analysis system using a remote web server with similar methods, but did not report on time consumption (the mean time necessary for segmentation 1h, and more in the case of calcifications). In our study, the time required for sizing, including segmentation and measurements, proved more appropriate for surgeons' expectations. Lee et al.¹⁷ have recently proposed the TeraRecon Aquarius workstation, using the same reconstructions as described above, but without clinical evaluation. Currently, most of the semi-automatic software used for sizing requires powerful hardware, and thus cannot be used by all vascular surgeons performing EVAR. Endosize software is aimed at fulfilling the surgeons' specific expectations, allowing for total autonomy in the forward planning of EVAR. This is achieved by using a mobile and user-friendly tool, which is able to run on a personal computer, unlike other software. Moreover, this tool has a quick learning curve and requires little time, which is the landmark of semi-automatic software¹⁸.

Our data suggests that the accuracy of the different lengths and diameters determined using Endosize prior to EVAR may be as reliable as that obtained with conventional radiological equipment. To plan EVAR, surgeons have a powerful new tool, which is more suitable than software currently used in clinical evaluations. Preoperative assessment prior to EVAR appears reliable, though peroperative

complications may occur with no warning. Further studies are necessary to assess the peroperative value of an angionavigation computer system in order to secure the placement of aortic stent grafts in 3D, and for more precise control over the deployment of different branches.

Acknowledgements:

The authors thank Dr. JF Heautot, Dr. A. Larralde and Dr. A. Roux from the radiology unit for their contributions.

This work was partially supported by French institutional grants (French National Research Agency (ANR) Through TecSan program (project ANGIOVISION n°ANR-09-TECS-003)).

References:

- 1 . Diehm N , Baumgartner I , Silvestro A . Automated software supported versus manual aorto-iliac diameter measurements in CT angiography of patients with abdominal aortic aneurysms: assessment of inter- and intraobserver variation . *Vasa* . 2005 ; 34 : 255 - 261
- 2 . Boll DT , Lewin JS , Duerk JL . Assessment of automatic vessel tracking techniques in preoperative planning of transluminal aortic stent graft implantation . *J Comput Assist Tomogr* . 2004 ; 28 : 278 - 285
- 3 . Haigron P , Bellemare ME , Acosta O . Depth-map-based scene analysis for active navigation in virtual angioscopy . *IEEE Transactions on Medical Imaging* . 2004 ; 23 : 1380 - 90
- 4 . Fleureau J , Garreau M , Simon A . Assessment of global cardiac function in MSCT imaging using fuzzy connectedness segmentation . *Computers In Cardiology* . 2008 ;
- 5 . Boldak C , Rolland Y , Toumoulin C . An improved model-based vessel tracking algorithm with application to computed tomography angiography . *Journal of Biocybernetics and Biomedical Engineering* . 2003 ; 23 : 41 - 63
- 6 . Singh K , Jacobsen BK , Solberg S . Intra- and interobserver variability in the measurements of abdominal aortic and common iliac artery diameter with computed tomography. The Tromsø study . *Eur J Vasc Endovasc Surg* . 2003 ; 25 : 399 - 407
- 7 . Dillavou ED , Buck DG , Muluk SC . Two-dimensional versus three-dimensional CT scan for aortic measurement . *J Endovasc Ther* . 2003 ; 10 : 531 - 8
- 8 . Shin CK , Rodino W , Kirwin JD . Can preoperative spiral CT scans alone determine the feasibility of endovascular AAA repair? A comparison to angiographic measurements . *J Endovasc Ther* . 2000 ; 7 : 177 - 183
- 9 . Parker MV , O'Donnell SD , Chang AS . What imaging studies are necessary for abdominal aortic endograft sizing? A prospective blinded study using conventional computed tomography, aortography, and three-dimensional computed tomography . *J Vasc Surg* . 2005 ; 41 : 199 - 205
- 10 . Sproule LR , Meier GH , Parent FN . Is three-dimensional computed tomography reconstruction justified before endovascular aortic aneurysm repair? . *J Vasc Surg* . 2004 ; 40 : 443 - 447
- 11 . Velazquez OC , Woo EY , Carpenter JP . Decreased use of iliac extensions and reduced graft junctions with software-assisted centerline measurements in selection of endograft components for endovascular aneurysm repair . *J Vasc Surg* . 2004 ; 40 : 222 - 227
- 12 . Cayne NS , Veith FJ , Lipsitz EC . Variability of maximal aortic aneurysm diameter measurements on CT scan: significance and methods to minimize . *J Vasc Surg* . 2004 ; 39 : 811 - 815
- 13 . Isokangas JM , Hietala R , Perälä J . Accuracy of computer-aided measurements in endovascular stent-graft planning: an experimental study with two phantoms . *Invest Radiol* . 2003 ; 38 : 164 - 170
- 14 . Aziz I , Lee J , Lee JT . Accuracy of three-dimensional simulation in the sizing of aortic endoluminal devices . *Ann Vasc Surg* . 2003 ; 17 : 129 - 136
- 15 . Fukuhara R , Ishiguchi T , Ikeda M . Evaluation of abdominal aortic aneurysm for endovascular stent-grafting with volume-rendered CT images of vessel lumen and thrombus . *Radiat Med* . 2004 ; 22 : 332 - 341
- 16 . Neri E , Bargellini I , Rieger M . Abdominal aortic aneurysms: virtual imaging and analysis through a remote web server . *Eur Radiol* . 2005 ; 15 : 348 - 352
- 17 . Lee WA . Endovascular abdominal aortic aneurysm sizing and case planning using the TeraRecon Aquarius workstation . *Vasc Endovascular Surg* . 2007 ; 41 : 61 - 67
- 18 . Boll DT , Lewin JS , Duerk JL . Assessment of automatic vessel tracking techniques in preoperative planning of transluminal aortic stent graft implantation . *J Comput Assist Tomogr* . 2004 ; 28 : 278 - 285

Fig. 1

AAA morphometry: diameters and length measurements

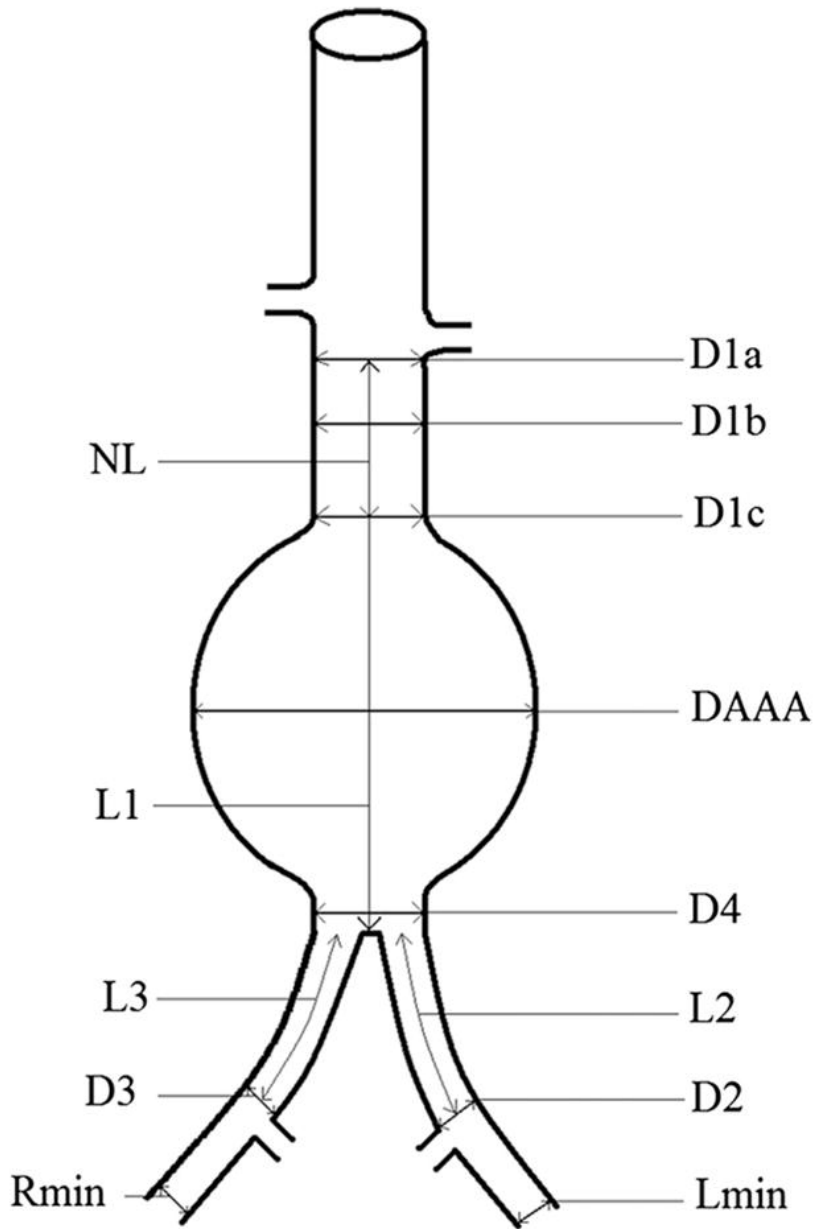


Fig. 2

Semi-automatic sizing step: Diameters are measured on a 3D image perpendicular to the aorto-iliac centerline (slice located on the right side interface)

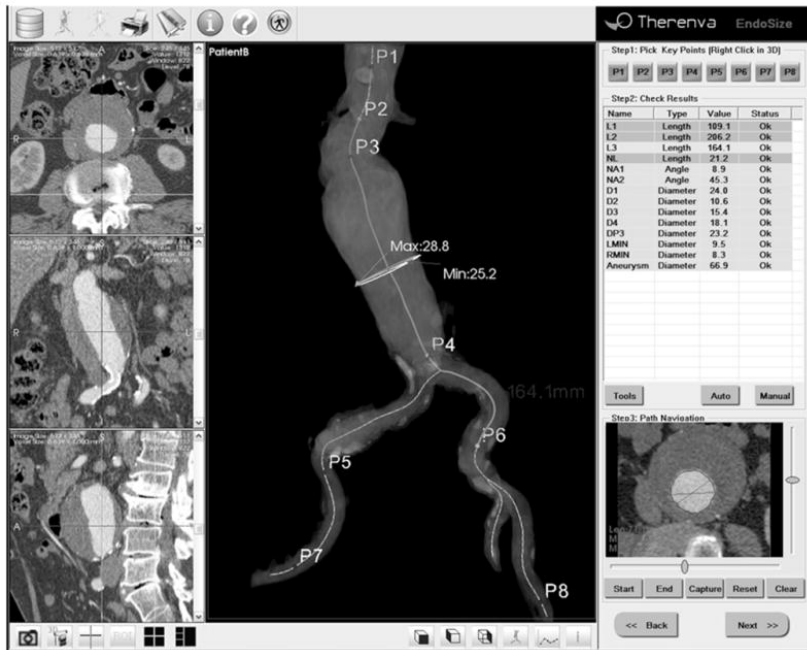


Fig 3

Sizing report: Criteria with a status that is not "OK" may be a contraindication for EVAR

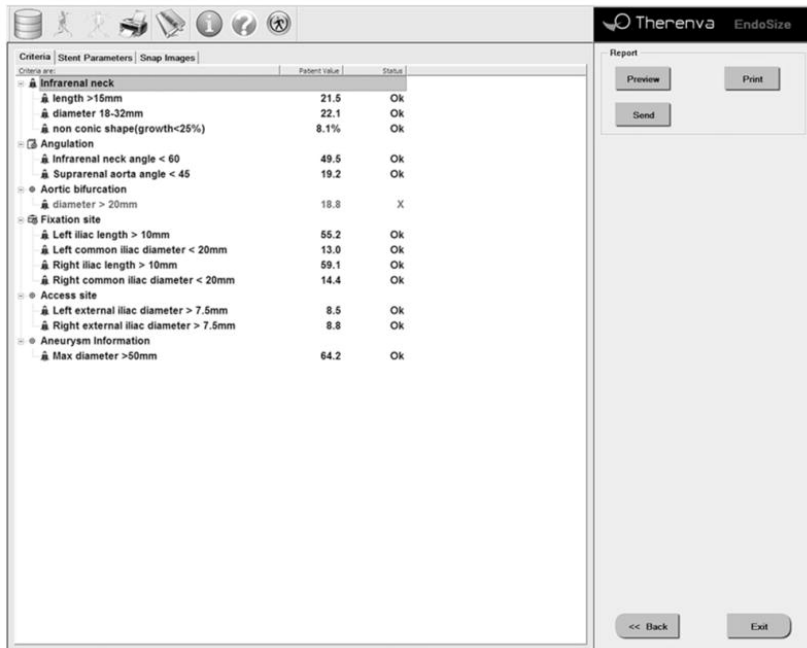


Fig. 4

ICCs based on comparisons of surgeons' measurements (intra- and inter-observer) using Endosize and those of the radiologist (Advance vessel analysis) and surgeons (Endosize)

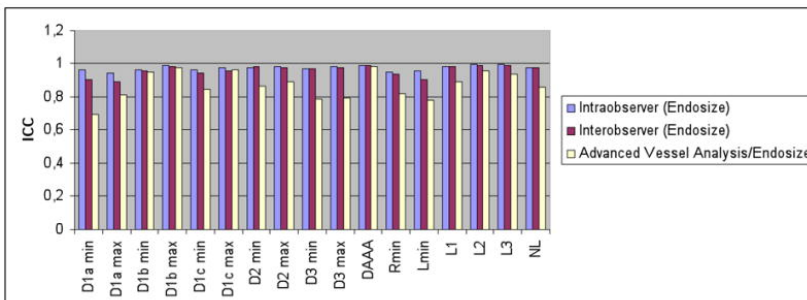


Fig 5

a,b,c. Difference between measurements taken using AVA and Endosize. Bland Altman plots for D1a, Rmin, and L3 are presented

Fig. 5a

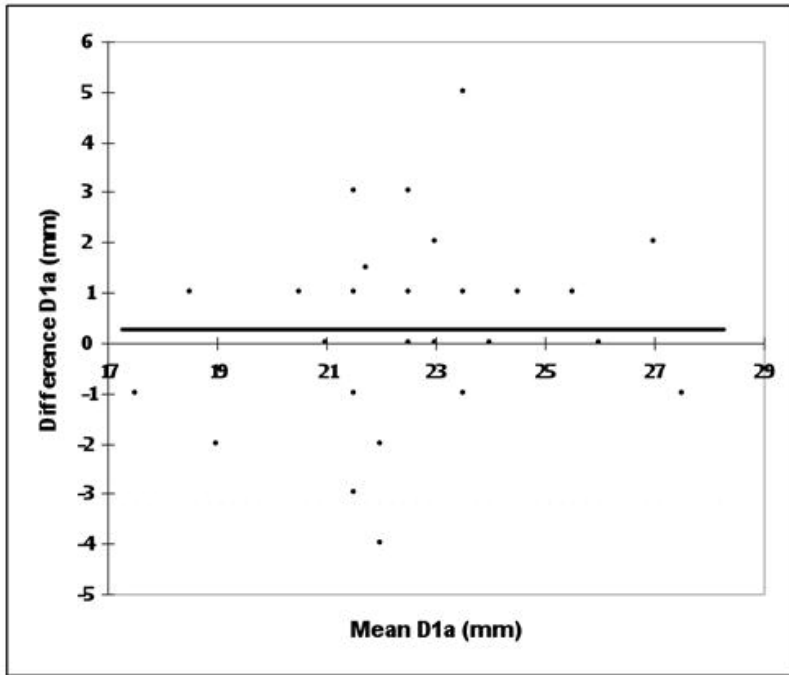


Fig. 5b

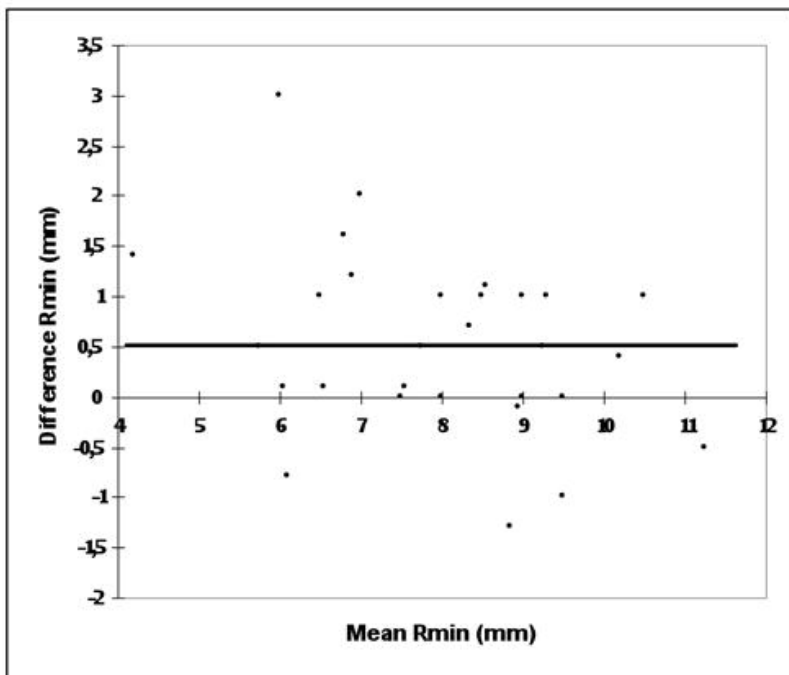


Fig. 5c

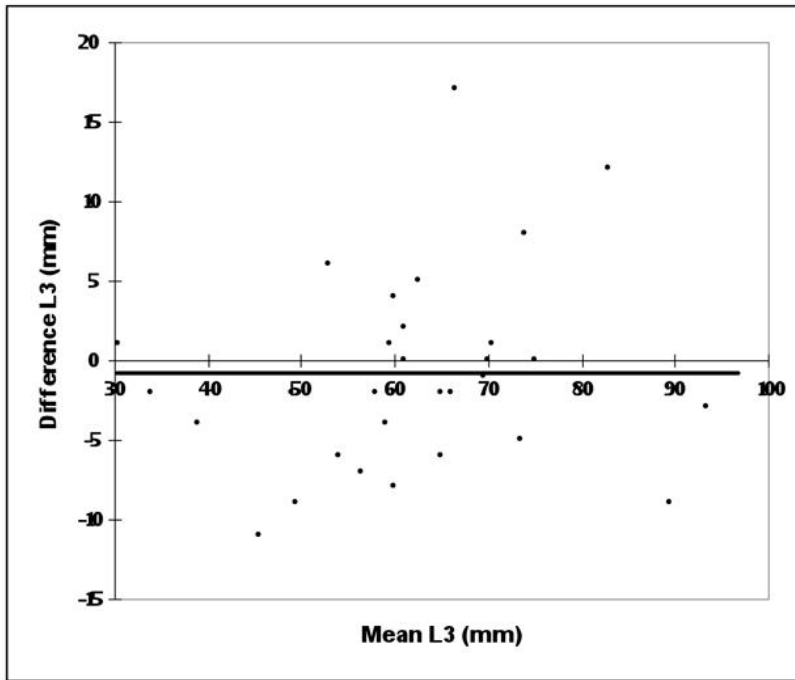


Table 1

Patient selection criteria for EVAR and morphological characteristics of AAA not selected for EVAR

Inclusion Clinical Criteria

Age>80 years
 Non revascularizable coronary arterial disease
 Cardiac insufficiency with clinical signs
 Non-operable aortic stenosis
 Left ventricular ejection fraction<40%
 Severe chronic respiratory insufficiency
 Plasmatic creatinine>200uL/L
 Hostile abdomen

Exclusion Morphological Criteria

Neck length \leq 15mm
 Circular thrombus or calcifications at stent graft
 Fixation sites
 Bony sharp neck \geq 60°
 Iliac tortuosity \geq 80°

Table 2

Intra-observer correlation, variation, and absolute differences

	ICC	Mean difference (mm)	Lower agreement limit	Upper agreement limit	Absolute difference \leq 2mm	Absolute difference \leq 5mm
D1a min	0.963	0.469	-0.16	0.77	100%	100%
D1a max	0.944	0.438	-0.48	0.39	98.4%	100%
D1b min	0.966	0.578	-0.38	0.77	98.3%	100%
D1b max	0.989	0.319	-0.36	0.23	100%	100%
D1c min	0.967	0.563	-0.57	0.56	96.9%	100%
D1c max	0.979	0.516	-0.59	0.44	96.9%	100%
D2 min	0.978	0.633	-0.48	0.78	95.3%	100%
D2 max	0.982	0.586	-0.28	0.88	98.4%	100%
D3 min	0.973	0.586	-0.53	0.64	95.3%	100%
D3 max	0.983	0.477	0.54	0.41	96.9%	100%
DAAA	0.993	0.881	0.11	1.82	96.9%	100%
Rmin	0.95	0.314	-0.12	0.5	100%	100%
Lmin	0.958	0.256	-0.1	0.41	100%	100%
L1	0.982	1.914	-0.58	3.19	73.4%	95.3%
L2	0.995	1.281	0.18	2.69	87.5%	100%
L3	0.994	1.344	0.04	2.67	81.3%	100%
NL	0.974	1.375	-0.48	2.23	85.9%	95.3%

AAA: abdominal aortic aneurysm, min: smallest diameter, max: largest diameter

ICC: intraclass correlation coefficient

Table 3

Inter-observer correlation, variation, and absolute differences

	ICC	Mean difference (mm)	Lower agreement limit	Upper agreement limit	Absolute difference ≤2mm	Absolute difference ≤2mm
D1a min	0.906	0.469	-0.16	0.77	95.3%	100%
D1a max	0.891	0.75	-0.32	1.16	92.2%	100%
D1b min	0.955	0.647	-0.38	0.78	98.3%	100%
D1b max	0.984	0.422	-0.39	0.45	98.3%	100%
D1c min	0.947	0.844	-0.30	1.37	92.2%	100%
D1c max	0.959	0.797	-0.39	1.19	93.8%	100%
D2 min	0.982	0.695	0.07	1.43	96.9%	100%
D2 max	0.979	0.648	-0.26	1.03	98.4%	100%
D3 min	0.969	0.759	-0.13	1.37	98.4%	100%
D3 max	0.977	0.695	-0.28	1.09	95.3%	100%
DAAA	0.993	0.909	0.03	1.80	93.8%	100%
Rmin	0.938	0.348	-0.12	0.56	100%	100%
Lmin	0.905	0.444	0.02	0.89	100%	100%
L1	0.982	2.051	-0.2	3.82	68.8%	83.8%
L2	0.99	1.94	0.62	4.39	70.3%	96.8%
L3	0.989	1.719	-0.22	3.16	71.9%	96.9%
NL	0.974	1.625	0.34	3.5	79.7%	96.6%

Table 4

Correlation, variation, and absolute differences between the two methods of measurements (Advanced vessel analysis/Endosize)

	ICC	Mean difference (mm)	Lower agreement limit	Upper agreement limit	Absolute difference $\leq 2\text{mm}$	Absolute difference $\leq 5\text{mm}$
D1a min	0.697	1.625	0.49	5.88	77.3%	99.2%
D1a max	0.813	0.969	-0.21	1.70	89.8%	100%
D1b min	0.948	0.806	-0.35	1.24	98.4%	100%
D1b max	0.974	0.573	-0.32	0.82	98.3%	100%
D1c min	0.846	1.52	-1.05	1.98	80.5%	95.3%
D1c max	0.963	0.83	-0.22	1.42	93.0%	100%
D2 min	0.864	1.865	-0.39	3.28	73.4%	92.2%
D2 max	0.89	1.688	0.05	3.36	86.6%	92.2%
D3 min	0.784	2.094	-0.46	3.67	70.3%	93.8%
D3 max	0.792	1.91	-0.91	2.87	74.2%	90.6%
DAAA	0.983	1.392	0.06	2.79	80.5%	99.2%
Rmin	0.821	0.711	0.05	1.44	96.1%	100%
Lmin	0.78	0.836	0.06	1.7	92.2%	100%
L1	0.892	3.974	-3.54	4.39	55.5%	89.5%
L2	0.956	3.875	0.05	7.64	49.2%	74.2%
L3	0.939	3.797	0.38	7.8	48.8%	76.6%
NL	0.86	3.39	-0.09	6.56	52.3%	82%

Table 5

Mean time, standard deviation, and minimum and maximum for one sizing with Endosize

Patient	mean time (min)	min	max
First sizing			
Surgeon 1	13.13+/-3.4	7.2	25.7
Surgeon 2	14.29+/-5.1	7.3	32.7
Second sizing			
Surgeon 1	11.57+/-4.08	7.3	23.9
Surgeon 2	13.38+/-4.64	7.8	29.8
Total	13.1+/-4.53	7.2	32.7

Table 6

Patients with an aorto-uni-iliac stent graft: alarms emitted by radiologist and surgeon.

Patient	Radiologist alarms	Surgeon alarms
A	V3, V5	V3, V5
B	V5	V5
C	V1, V4, V5, V8, V9	V1, V4, V5, V8, V9
D	V9, V11	V9
E	V1, V10	V1, V10

NL ≤ 15 mm (V1), D1a ≤ 18 mm or ≥ 32 mm (V2), reverse taper neck (or difference between D1a and D1c $\geq 25\%$) (V3), bony-sharp neck $\geq 60^\circ$ (V4), D4 ≤ 20 mm (V5), L2 ≤ 10 mm (V6), L3 ≤ 10 mm (V7), Lmin ≤ 7.5 mm (V8), Rmin ≤ 7.5 mm (V9), D2 ≥ 20 mm (V10), D3 ≥ 20 mm (V11)